

Received July 14, 2020, accepted July 24, 2020, date of publication July 29, 2020, date of current version August 12, 2020.

Digital Object Identifier 10.1109/ACCESS.2020.3012878

# Multi-Objective Topological Optimization of an Electric Truck Frame Based on Orthogonal Design and Analytic Hierarchy Process

JIE QIAO<sup>1</sup>, FENGXIANG XU<sup>2,3</sup>, KUNYING WU<sup>2,3</sup>, SUO ZHANG<sup>2,3</sup>, AND YONGTAO LIU<sup>1</sup>

<sup>1</sup>School of Automobile, Chang'an University, Xi'an 710064, China

<sup>2</sup>Hubei Key Laboratory of Advanced Technology of Automotive Components, Wuhan University of Technology, Wuhan 430070, China

<sup>3</sup>Hubei Collaborative Innovation Center for Automotive Components Technology, Wuhan University of Technology, Wuhan 430070, China

Corresponding author: Fengxiang Xu (xufx@whut.edu.cn)

This work was supported in part by the National Nature Science Foundation under Grant 51278062, Grant 51975438, and Grant U1564202; in part by the 111 Project under Grant B17034; and in part by the Fundamental Research Funds for the Central Universities in China under Grant 300102220111.

**ABSTRACT** The electric truck frame as a vital load-bearing component has aroused growing attentions due to its enormous potential in lightweight. However, few systematic studies have been performed on the multi-objective topological design of the frame attributable to its complexity on loading and conflicting objectives. This paper aims to develop a multi-objective topology optimization strategy of the electric truck frame based on the hybrid decision making method combining orthogonal test design (OTD) and analytic hierarchy process (AHP). The hybrid strategy is performed to obtain a new set of weight ratio combination from objective data and subjective judgment. The topological results show that the overall performance of the optimal frame is better than any of the methods applied alone. By comparing, it is found that the strength and stiffness of the optimal frame is higher than that of the original frame from the perspective of static conditions, and the low-order natural frequency of the optimal frame is significantly improved. It demonstrates that the proposed approach could be as an effective tool for multi-objective topology optimization of the electric truck frame in seeking lightweight and comprehensive mechanical performance. The hybrid strategy might be expected to provide some guidance for more complicated engineering problems.

**INDEX TERMS** Electric truck frame, multi-objective design, topology optimization, orthogonal test, analytic hierarchy process.


## NOMENCLATURE

$\mathbf{K}$	global stiffness matrix
$\mathbf{U}$	displacement vectors
$u_i$	displacement vectors of the $i$ th individual element
$k_0$	element stiffness matrix
$V$	the volume of the structure
$V^*$	the prescribed volume of the structure
$m$	total number of loading conditions
$\omega_k$	the weight value of the $k$ th working condition
$q$	penalty exponent
$C_k^{\max}$	the maximum value corresponding the $k$ th single objective
$C_k^{\min}$	the minimum value corresponding the $k$ th single objective

$\lambda_j$	the eigenvalue corresponding to the $i$ th eigenfrequency
$R_x$	the influence degree of the factor $x$ .
$\mathbf{M}$	the positive reciprocal matrix
$CI$	coincidence indicator

## I. INTRODUCTION

The frame subjected to various conditions such as bending and torsion during driving is the main load-bearing component of the whole vehicle, thereby it has aroused extensive research in term of the desirable balance between performances and lightweight [1]–[3]. While achieving weight reduction could not sacrifice stiffness, the low-order natural frequencies should be maximized to avoid resonances caused by excitations from the transmission system, engine vibration or uneven road surfaces [3], [4]. Therefore, it is necessary to develop a multi-objective optimization function to achieve the

The associate editor coordinating the review of this manuscript and approving it for publication was Mouloud Denai .

minimum mean-compliance of multi-conditions under and maximize eigenfrequency under dynamics [5], [6].

For the multi-objective optimization problem, the classical method is to simply transform the multi-objective problem into a single-objective problem by linear weighted sum method. Although this method is simple to calculate, it is quite difficult to solve all Pareto optimal solutions for nonconvex optimization problems [7], [8]. In recent years, a multi-objective topology optimization method based on compromise programming theory has been widely used by researchers [9]–[11]. However, it might be unreasonable for designers to directly assign values for weights because of the uncertain, incomplete, and local properties inherent to weights themselves [12].

In multi-objective optimization, the weight-to-weight ratio between sub-goals will directly affect the outcome of the composite objective function. Therefore, how to reasonably allocate the weight value of multi-objective optimization neuron target is a problem worthy of exploration. To sum up the previous studies, the weighting method can be divided into two categories from subjective judgment and objective calculation.

In view of the objective weighting method, Zhang *et al.* [13] proposed a method for determining the weight factors of the sub objective of the comprehensive objective function by grey comprehensive relational analysis. The sub sequences obtained by single objective topology and optimal sequence formed by each objective optimal value were exerted comprehensive relational analysis to obtain the weight factors. Li and Wang [14] proposed a  $\alpha$ -method to determine the weighting factors under various working conditions whose basic principle was to construct a hyperplane equation through the optimal solution of each working condition. Qin and Yang [15] utilized the expert evaluation method to acquire the grey interval of the operating condition weight coefficient, and then calculated the exact value of the grey interval of the operating condition weight coefficient by combining the grey theory. Other researchers [16]–[18] combined the weight coefficients by orthogonal table, and analyzed the test results by the range analysis method to obtain the optimal weight ratio coefficient. The above methods for calculating weights acquire original information from an objective environment, and there is no subjective judgment of researchers. Therefore, those methods do not take into account the relative importance of each sub-goal in the actual project, and the target weight is completely different from the relative importance of each target in the actual project.

Fortunately, the subjective weighting method is drove to solve this issue. In some literatures, the designer directly determines the importance of all working conditions according to own experience, and gives a ratio as the weight coefficient [19]–[21]. Ryu *et al.* [22] proposed a multi-objective optimization method using an adaptive weight determination scheme and tunneling method. To find the optimum designs that are evenly distributed on the Pareto front, the weights of different objective functions are adaptively determined by

using the concept of a hyperplane so that new solutions can be gradually found in the objective space. Marler and Arora [23] determined the factors that dictate which solution point results from a particular set of weights and fundamental deficiencies are identified in terms of a priori articulation of preferences, and guidelines are provided to help avoid blind use of the method. Sato *et al.* [24] proposed a new Pareto frontier exploration methodology for multi-objective topology optimization problems by using a population-based approach in which multiple points in the objective space are updated and moved to the Pareto frontier.

Regarding multi-objective decision-making methods, the extension to multi-objective optimization design has been extensively studied. These methods are substantial and diverse, but they all seek solutions based on the correlation between the data. The principal component analysis (PCA) [25], as one of the multi-objective decision-making methods, is to explain the structure of variance-covariance by using the linear combination of each response quality feature, which is used to analyze the degree of influence of different responses on the system. In addition, in the gray entropy theory, the larger the entropy value is, the greater the disturbance of the corresponding response is. The gray entropy measurement method is also a method for evaluating the importance of each response in a multi-response system [26]. Furthermore, the TOPSIS method is also an important multi-objective decision-making method. It determines the current object's pros and cons by calculating the relative fit between the current point and the optimal and worst solutions. Amit Kumar Singh *et al.* [27] proposed a fuzzy-AHP and TOPSIS based approach for selection of composite materials used in structural applications, which has been used for calculating the weights of mechanical properties and for ranking of different alternate composite materials respectively.

At present, according to the data determining the weight coefficient is derived from subjective judgment and calculated objectively, the weighting method can be divided into two categories: subjective weighting method and objective weighting method. The basic principle of the subjective weighting method is that researchers select the weight value of each target reasonably according to the relative importance of each condition or performance in the actual project and combine with experience. The advantage of the method is that the weight of the target is consistent with the actual importance of the target. However, the results are subjective and arbitrary, lacking certain objectivity, and the results are not necessarily optimal. The objective weighting method calculates the weight data by obtaining the original information from the objective environment. There is no subjective judgment of the researchers, and the objectivity is strong. However, the relative importance of each sub-goal in actual engineering is not taken into consideration. The weight coefficient of the goal often obtained is opposite to the relative importance of each goal in actual engineering.

Different from other scholars' constructive works with only subjective weighting method or only objective weighting

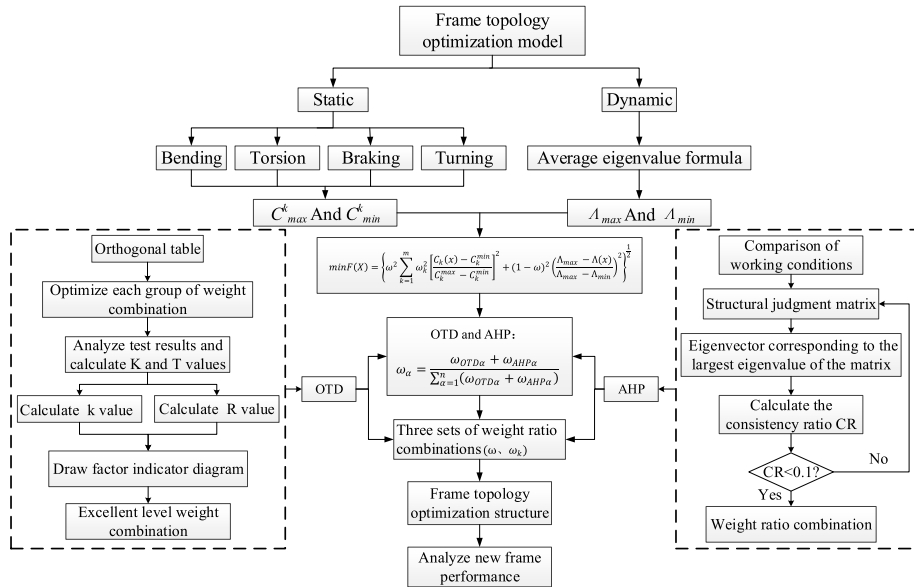


FIGURE 1. Flowchart of multi-objective topological optimization of an electric truck frame based on orthogonal test and analytic hierarchy process.

method, this study aims to develop a hybrid method to effectively determine weight values combining with objective and subjective weighting method. In other words, this paper aims to develop a topology optimization strategy of dynamic electric truck frame based on orthogonal test design (OTD) and analytic hierarchy process (AHP). The results show that the comprehensive performance of the obtained frame topology is better than that obtained by the respective corresponding method alone therein. Compared with that of the original frame, it is found that the strength of the new frame is higher than that of the original frame. Importantly, the low-order natural frequency of the new frame is significantly improved, which demonstrate that the proposed approach could be an effective tool for topology optimization of the electric truck frame. The proposed coupling method is expected to provide some guidance for more complicated engineering problems in similar structural design.

## II. MULTI-OBJECT TOPOLOGY OPTIMIZATION STRATEGY OF AN ELECTRIC TRUCK FRAME

### A. OPTIMIZATION FLOWCHART

The most significant contribution of this paper is the further development of multi-objective topology optimization inspired by multi-objective decision making method. Specifically, a multi-objective decision-making method coupling OTD and AHP to guide the multi-objective topology optimization design of structures is proposed considering the sensitivity of weight ratios of conflicting objectives to optimization results.

The detailed flowchart concerning multi-objective topology optimization design of a frame is shown in Figure 1. First, a finite element model of an electric truck frame is established, as well the optimized and non-optimized areas

are defined. Then, a compromised programming method is applied to establish a multi-objective topology optimization mathematical model for the frame by combining static stiffness and dynamic natural frequency. Further, the weight ratios for optimization objectives are calculated according to the OTD, AHP and the two coupling methods. Finally, the multi-objective decision method is introduced into the multi-objective topology optimization to guide the design of weight ratio for complex and contradictory functions, so as to obtain a desirable design scheme for lightweight and comprehensive mechanical performance of the electric truck frame.

### B. MULTI-OBJECTIVE TOPOLOGY OPTIMIZATION METHOD

Structural topology optimization subjected to static load with multiple conditions is to study the optimal distribution of materials in the design domain to minimize structural compliance (i.e. maximum stiffness). Taking compliance minimization as the objective, the density of the structure unit as the design variable and the volume fraction as the constraint condition, the mathematical model of single-condition topology optimization based on the solid isotropic material with penalization theory (SIMP) is described as follows [28]–[31]:

$$\begin{cases} \text{find } X = [x_1, x_2, \dots, x_n]^T \in R^n \\ \min C(X) = U^T K U = \sum_{i=1}^n E_i(x_i) u_i^T k_0 u_i \\ \text{s.t. : } V(X) - V^* \leq 0 \\ 0 \leq x_{\min} \leq x_i \leq 1 \end{cases} \quad (1)$$

where  $K$  and  $U$  are the global stiffness matrix of the structure and displacement vectors, respectively.  $F$  refers to the force vector of this system. The design variable  $x_i$  denotes the density of  $i$ th element.  $u_i$  represents the displacement vectors

of the  $i$ th individual element,  $k_0$  is the element stiffness matrix of structure before optimization.  $V$  and  $V^*$  represent the volume and prescribed volume of the structure, respectively. To obtain a solid-void design, two bound densities ( $1$  and  $x_{\min}$ ) are defined as discrete design variables. A minimum value of  $x_{\min}$  denotes the void elements; effectively avoid the singularity of the stiffness matrix.

For topological optimization design of structure, only one corresponding topological structure can be obtained under one load condition. However, in practical engineering, the frame needs to satisfy multiple working conditions at the same time, which might involve multi-objective decision making. In order to achieve the desirable Pareto optimal solution, a multi-objective topological optimization function based on compromise programming approach can be defined as [11], [32], [33]:

$$\min C(X) = \left\{ \sum_{k=1}^m \omega_k^q \left[ \frac{C_k(x) - C_k^{\min}}{C_k^{\max} - C_k^{\min}} \right]^q \right\}^{\frac{1}{q}} \quad (2)$$

where  $m$  refers to the total number of loading conditions,  $\omega_k$  represents the weight value of the  $k$ th working condition.  $q$  is a penalty exponent ( $q \geq 2$ ), and here  $q$  is set as 2.  $C_k(x)$  denotes the objective related to the  $k$ th loading case and  $C_k^{\max}$  and  $C_k^{\min}$  are the maximum value and minimum value corresponding the  $k$ th single objective in the feasible region.

The frame is not only subjected to static loads, but also to the excitation of dynamic external loads. Therefore, the topological optimization of dynamic vibration frequency is introduced to improve the low order frequency of the frame and avoid resonance phenomenon. Unfortunately, as maximizing the  $i$ th eigenfrequency,  $(i + 1)$ th or  $(i - 1)$ th eigenfrequency may fall down to the lower value, and the eigenfrequencies switch their orders very frequently in the optimization process, which may result in divergence of the optimization problem. In order to overcome the defect, mean-frequency formulation has been suggested as seen below [34], [35]:

$$\max \Lambda(X) = \lambda_0 + s \left( \sum_{j=1}^f \frac{\omega_j}{\lambda_j - \lambda_0} \right)^{-1} \quad (3)$$

where  $\lambda_j$  represents the specified eigenvalues.  $\lambda_j$  refers to the eigenvalue corresponding to the  $i$ th eigenfrequency.  $\omega_j$  denotes the given weighting coefficients.  $\lambda_0$  and  $s$  are arbitrary constants, used for generating some physical meaning of the objective function and adjusting its dimension.

It is extremely necessary to consider the topology optimization of the frame structure under both static and dynamic conditions. It is worth noting that the attribute difference between stiffness and frequency requires standardization of each sub-goal to eliminate the influence of different sub-goal attributes on the comprehensive objective function. Therefore, combining formula (2) and formula (3), a new multi-objective topology optimization model of frame

structure can be obtained as follows:

$$\min F(X) = \left\{ \omega^2 \sum_{k=1}^m \omega_k^2 \left[ \frac{C_k(x) - C_k^{\min}}{C_k^{\max} - C_k^{\min}} \right]^2 + (1 - \omega)^2 \left( \frac{\Lambda_{\max} - \Lambda(x)}{\Lambda_{\max} - \Lambda_{\min}} \right) \right\}^{\frac{1}{2}} \quad (4)$$

where  $F(X)$  represents the object function.  $\omega$  refers to the weight coefficient of the compliance objective function. The values of  $C_k^{\max}$ ,  $C_k^{\min}$ ,  $\Lambda_{\max}$  and  $\Lambda_{\min}$  can be acquired from the optimization results of equations Eq. (1) and Eq. (3), respectively.

### C. DECISION MAKING METHOD COMBINING OTD AND AHP

Orthogonal test design (OTD) is a scientific calculation method for efficiently dealing with multi-factor optimization problems attributable to its benefit in less experiment numbers than full-factor experiment [36]–[38]. In the orthogonal experiment, the standardized orthogonal table is applied to carry out the experimental scheme, and then the optimization scenario is performed based on the corresponding calculation and analysis.

Range analysis with the range defined as the distance between the extreme values of the data is a statistical method for determining the sensitivity of each factor to test results based on orthogonal experiments. The calculation process of range analysis is shown in Eq. (5) and Eq. (6) [39].

$$k_{xi} = \frac{K_{xi}}{4} \quad (5)$$

$$R_x = \max(k_{x1}, k_{x2}, k_{x3}, k_{x4}) - \min(k_{x1}, k_{x2}, k_{x3}, k_{x4}) \quad (6)$$

where  $K_{xi}$  stands for the sum of the experimental results which cover the factor  $x$  with  $i$  level.  $k_{xi}$  represents the average value of the test results at the same level.  $R_x$  means the influence degree of the factor  $x$ .

To verify the correctness of the analysis results, an indicator is introduced which represents the sum of all test results. The formula Eq. (7) indicates the sum of all the horizontal calculation results of each factor.

$$T = K_1 + K_2 + K_3 + K_4 \quad (7)$$

According to the experience and judgment of experts, a judgment matrix  $M = (M_{ij})_{n \times n}$  is constructed by comparing the relative importance of sub-items in the analytic hierarchy process (AHP). In the judgment matrix (Eq. (8)),  $n$  denotes the number of working conditions, and  $M_{ij}$  represent important degree of the  $i$ th working condition compared with the  $j$ th. The number (1~9) and its reciprocal can be used as the scale of the judgement matrix [40], [41], as shown in Table 1.

$$M = \begin{bmatrix} M_{11} & M_{12} & \cdots & M_{1n} \\ M_{21} & M_{22} & \cdots & M_{2n} \\ \vdots & \vdots & \dots & \vdots \\ M_{n1} & M_{n2} & \cdots & M_{nn} \end{bmatrix} \quad (8)$$

TABLE 1. Definition of the scale of the judgment matrix.

Intensity of importance	Explanation
1	$i$ is as important as $j$
3	$i$ is a little more important than $j$
5	$i$ is more important than $j$
7	$i$ is strongly more important than $j$
9	$i$ is extremely more important than $j$
2, 4, 6, 8	Represent the intermediate values of the above adjacent judgments
Reciprocals of above	If $i$ has one of the above nonzero numbers assigned to it when compared with $j$ , then $j$ has the reciprocal value when compared with $i$ . $M_{ji}=1/M_{ij}$

The matrix  $M$  has two characteristics: one is  $M_{ij} > 0$  and the other is  $M_{ji} = \frac{1}{M_{ij}}$  ( $j, i = 1, 2, \dots, n$ ).  $M$  refers to the positive reciprocal matrix in which  $M_{ii} = 1$ .

The eigenvectors  $\omega$  and the maximum eigenvalue  $\lambda_{max}$  of the judgment matrix are calculated according to the square root method [42], [43]:

$$\omega_i = \frac{\left(\prod_{j=1}^n M_{ij}\right)^{\frac{1}{n}}}{\sum_{i=1}^n \left(\prod_{j=1}^n M_{ij}\right)^{\frac{1}{n}}}, \quad i = 1, 2, \dots, n \quad (9)$$

$$\omega = [\omega_1, \omega_2, \omega_3, \dots, \omega_n]^T \quad (10)$$

$$\lambda_{max} = \frac{1}{n} \sum_{i=1}^n \frac{(M\omega)_i}{\omega_i} \quad (11)$$

where  $(M\omega)_i$  denotes the  $i$ th element of  $M\omega$ :

$$M\omega = \begin{bmatrix} (M\omega)_1 \\ (M\omega)_2 \\ \vdots \\ (M\omega)_n \end{bmatrix} = \begin{bmatrix} M_{11} & M_{12} & \dots & M_{1n} \\ M_{21} & M_{22} & \dots & M_{2n} \\ \vdots & \vdots & \dots & \vdots \\ M_{n1} & M_{n2} & \dots & M_{nn} \end{bmatrix} \begin{bmatrix} \omega_1 \\ \omega_2 \\ \vdots \\ \omega_n \end{bmatrix} \quad (12)$$

In general, if the positive reciprocal matrix  $M$  satisfies  $M_{ij} \cdot M_{jk} = M_{ik}$ ,  $i, j, k = 1, 2, \dots, n$ , then  $M$  is called the consistency matrix. In addition, the normalized eigenvector corresponding to the maximum eigenvalue of the judgment matrix is taken as the weight vector of all subitems in the objective function. However, there is a problem that the actual judgment matrix is usually inconsistent, which drives the calculation of CR (consistency ratio) and verifies whether the degree of inconsistency of matrix  $M$  is within the acceptable range according to the consistency judgment criterion.

$$CI = \frac{\lambda_{max} - n}{n - 1} \quad (13)$$

$$CR = \frac{CI}{RI} \quad (14)$$

where CI means coincidence indicator. When  $CI = 0$  ( $\lambda_{max} = n$ )  $M$  refers to a consistency matrix. The larger CI means the more inconsistent of the matrix  $M$ . RI indicates the random consistency index.

The topological structure obtained by OTD and AHP give full play to their respective advantages. Specifically, the weight combination obtained through OTD will make the comprehensive objective function reach the best without considering the relative importance of the framework under each working condition in the actual project. Although the weight ratio combination obtained by AHP fully is taken account of the relative importance of actual engineering conditions, the comprehensive objective function obtained was not the optimal value. Therefore, the hybrid strategy of the above two methods is developed to obtain a new set of weight ratio combination. That is to say, the determination of weight ratio not only comes from objective actual data, but also includes subjective judgment, which fully reflects the complementarity between subjective weighting method and objective weighting method. The new weight ratio combination can be obtained by the following formula:

$$\omega_\alpha = \frac{\omega_{OTD\alpha} + \omega_{AHP\alpha}}{\sum_{\alpha=1}^n (\omega_{OTD\alpha} + \omega_{AHP\alpha})} \quad (15)$$

where  $\omega_{OTD\alpha}$  and  $\omega_{AHP\alpha}$  represent the weight values of the  $\alpha$ -th working condition obtained by the OTD and by the AHP, respectively, and  $n$  refers to the number of all working conditions.

### III. NUMERICAL MODEL OF THE ELECTRIC TRUCK FRAME

In this paper, the geometry model of the electric truck frame is established and the outer dimensions of the frame are 5560 mm  $\times$  700(800) mm  $\times$  165 mm, as shown in Figure 2. It is mainly divided into two domains, i.e., the optimized area and the non-optimized area.

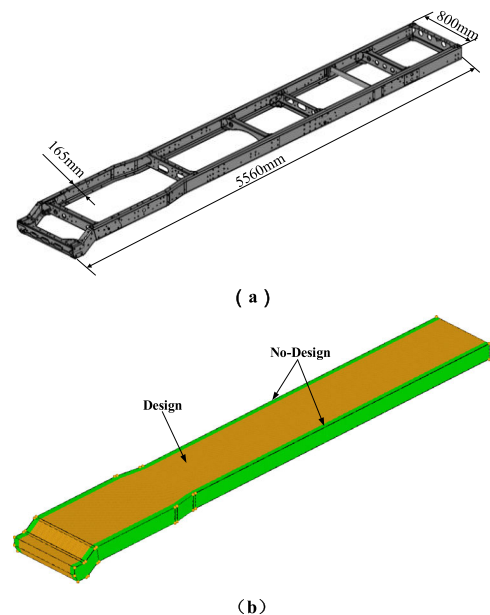


FIGURE 2. The geometry model of the electric truck frame.

Based on the geometry model, the finite element model of electric truck frame is shown in Figure 3. In order to ensure the accuracy of the optimization results and consider the efficiency of the optimization iteration, 10 mm × 10 mm × 10 mm hexahedral grid units were used to discretize the frame and the frame model was discretized into 760240 hexahedral units and 816534 nodes. The used material of the frame is 16Mn steel and its mechanical properties are shown in Table 2. The frame structure is subjected to the main load with the cab assembly 500 kg, cargo box 500 kg, rated load 2500 kg and battery assembly 320 kg. The cab is mounted at the front of the frame and the battery assembly is fixed on both side longitudinal beams. According to the actual loading situation of the frame, the cab and the battery assembly are simulated by the concentrated load and applied to the corresponding position of the longitudinal beam. The mass and rated loads of the container are distributed to the corresponding position of the stringers in the form of a uniform load with dynamic load factor 2 after full consideration of security.

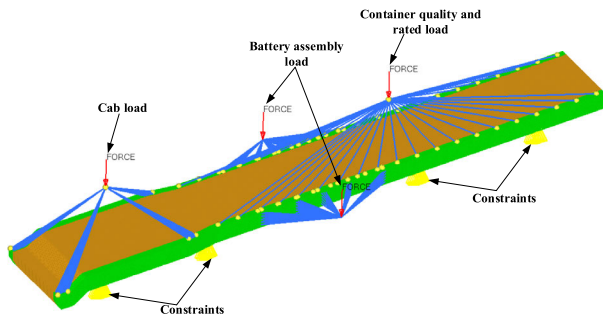


FIGURE 3. Finite element model of the electric truck frame.

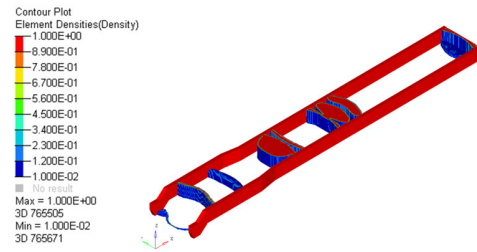
TABLE 2. The material properties of the electric truck frame.

Young's modulus (MPa)	Poisson's ratio	Density(t/mm3)	Yield limit (MPa)
$2.1 \times 10^5$	0.3	$7.8 \times 10^9$	345

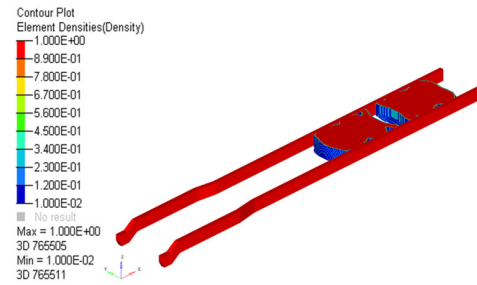
Herein, the four conditions would be considered, i.e., bending, torsion, braking and turning. Table 3 shows the constraints of each wheel under various working conditions. Among them, UX, UY and UZ represent the degree of freedom of displacement constrained by the X, Y and Z directions, respectively.

TABLE 3. The constraint conditions under each working case.

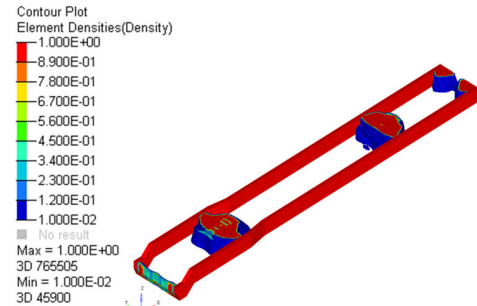
Conditions	Left front wheel	Right front wheel	Left rear wheel	Right rear wheel
Bending	UX, UZ	UX, UY, UZ	UZ	UX, UY, UZ
Torsion	UX, UY, UZ	UX, UZ	UZ(+5mm)	UZ (-5mm)
Braking	UX, UY, UZ	UX, UY, UZ	UX, UZ	UX, UZ
Turning	UX, UY, UZ	UX, UZ	UY, UZ	UY, UZ



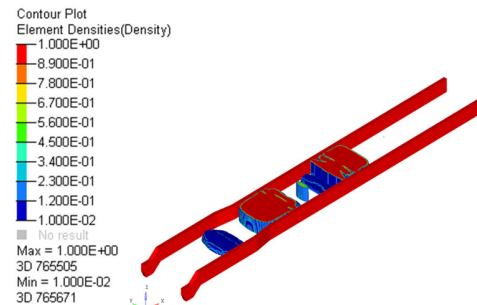
(a)



(b)



(c)



(d)

FIGURE 4. Topology optimization structure of frame under various working condition: (a) bending; (b) torsion; (c) braking; (d) turning.

## IV. RESULTS AND DISCUSSIONS

### A. SINGLE-OBJECTIVE TOPOLOGY OPTIMIZATION

The minimum mean compliance is the objective function of stiffness (Eq. (1)) and the maximum average frequency is taken as the objective function of the characteristic frequency (Eq. (3)). For the sake of getting an ideal frame topology, the maximum number of optimization iterations is defined as 80 and the minimum density of a unit is limited as 0.01. The volume fraction constraint is chosen to be 0.3. Topology optimization structure of frame under various working condition is illustrated in Figure 4. It can be seen that the

strain energy of the frame structure is reduced to different degrees under each working condition, but the frame topological structure can be optimized under different working conditions. The frame topology under each operating condition can only meet the operating requirements under this operating condition, but cannot be applied to other operating conditions. Therefore, it is necessary to combine all working conditions to carry out multi-objective topological optimization of the frame, so as to obtain a frame topological structure suitable for all working conditions. The compliance iteration curves are depicted in Figure 5(a), and it can be found that compared to the other cases where case 4 has the maximum compliance, case 1 has the minimum compliance. The mean eigenvalue basically converges in the fifth iteration, as shown in Figure 5(b). Combining the results of the static stiffness of frame under single working condition and the dynamic frequency optimization, the maximum and minimum compliance values under each working condition and mean-eigenvalue values are obtained and listed in Table 4.

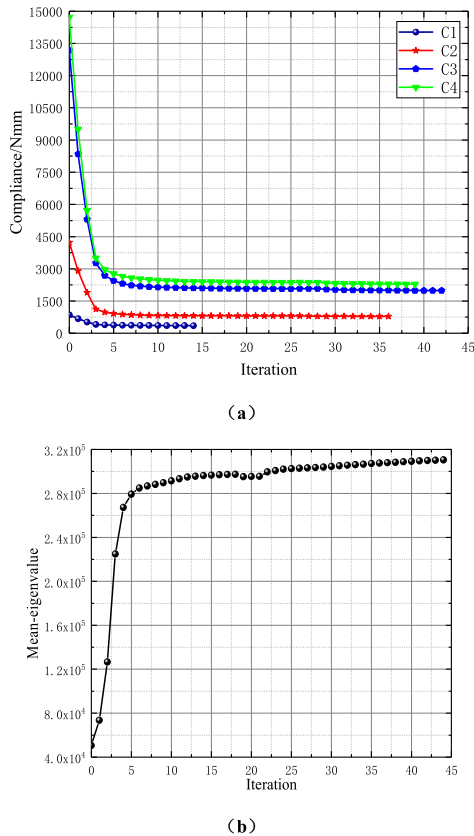


FIGURE 5. The compliance and frequency iteration curves: (a) Mean-compliance iteration curves; (b) Mean-eigenvalue iteration curve.

**B. MULTI-OBJECTIVE TOPOLOGY OPTIMIZATION**

According to the comprehensive optimization objective function (Eq. (4)), the weight coefficients are divided into two categories. One is the weight ratio coefficient between four working conditions of static stiffness, and another is the

TABLE 4. The optimal objective results of the frame under different conditions.

Cases	Bending	Torsion	Braking	Turning	Mean-eigenvalue
$C_{max}$	857	4226	13180	14720	-
$C_{min}$	353	783	1985	2286	-
$\Lambda_{max}$	-	-	-	-	310546
$\Lambda_{min}$	-	-	-	-	50594

weight ratio coefficient between the static stiffness and the dynamic frequency. Specifically, the weight values of four compliance cases and frequency in the comprehensive objective function are taken as the factor with 4 levels adding up to 1, as shown in Table 5.

TABLE 5. Design variables and corresponding candidate choices.

Factors	Description	Level1	Level2	Level3	Level4
A	Bending $\omega_1$	0.1	0.2	0.3	0.4
B	Torsion $\omega_2$	0.2	0.3	0.4	0.1
C	Braking $\omega_3$	0.3	0.4	0.1	0.2
D	Turning $\omega_4$	0.4	0.1	0.2	0.3
E	Static stiffness $\omega$	0.3	0.4	0.5	0.6

A total of 16 frame topology optimization design tests presented in orthogonal table  $L_{16}(4^5)$  is calculated by Eq. (4) to obtain the response as shown in Table 6. It can be seen from the values of each group of  $F(X)$  that the results obtained

TABLE 6. Orthogonal test results.

Scenario	A	B	C	D	E	F(X)
1	0.10	0.20	0.30	0.40	0.30	0.2064
2	0.11	0.33	0.44	0.11	0.40	0.2103
3	0.13	0.5	0.13	0.25	0.50	0.2125
4	0.14	0.14	0.29	0.43	0.60	0.1804
5	0.20	0.20	0.40	0.20	0.60	0.1812
6	0.18	0.27	0.27	0.27	0.50	0.2067
7	0.17	0.33	0.17	0.33	0.40	0.2116
8	0.40	0.20	0.20	0.20	0.30	0.2119
9	0.33	0.22	0.11	0.33	0.40	0.2262
10	0.30	0.30	0.20	0.20	0.30	0.2005
11	0.27	0.36	0.27	0.09	0.60	0.1871
12	0.25	0.08	0.33	0.33	0.50	0.2091
13	0.44	0.22	0.22	0.11	0.50	0.2179
14	0.33	0.25	0.08	0.33	0.60	0.1898
15	0.27	0.27	0.27	0.20	0.30	0.1995
16	0.40	0.10	0.30	0.20	0.40	0.2380
K1	0.8096	0.8317	0.8382	0.8169	0.8183	-
K2	0.8114	0.8073	0.8001	0.8272	0.8861	3.2891
K3	0.8229	0.8107	0.8404	0.8322	0.8462	-
K4	0.8452	0.8394	0.8104	0.8128	0.7385	-
k1	0.2024	0.2079	0.2096	0.2042	0.2046	-
k2	0.2029	0.2018	0.2000	0.2068	0.2215	-
k3	0.2057	0.2027	0.2101	0.2081	0.2116	-
k4	0.2118	0.2099	0.2026	0.2032	0.1846	-
R	0.0094	0.0081	0.0101	0.0049	0.0369	-

by combining optimization with different weight ratios are somewhat different.

According to the  $k_{X_i}$  presented in Table 6, the relationship between factors and levels can be illustrated in Figure 6, from which the influence degree of each factor on the test results at all levels can be intuitively seen. To minimize the comprehensive objective function, the level of each factor that minimizes the average should be chosen. According to Figure 6, it can be seen that the optimal level combination to minimize the value of the comprehensive objective function is A1, B2, C2, D4, E4. After normalization, the combination of weight ratio determined by orthogonal test design to achieve the optimal comprehensive objective can be obtained as follows:  $\omega_{OTD1} = 0.091, \omega_{OTD2} = 0.273, \omega_{OTD3} = 0.363, \omega_{OTD4} = 0.273, \omega_{OTD} = 0.600$ .

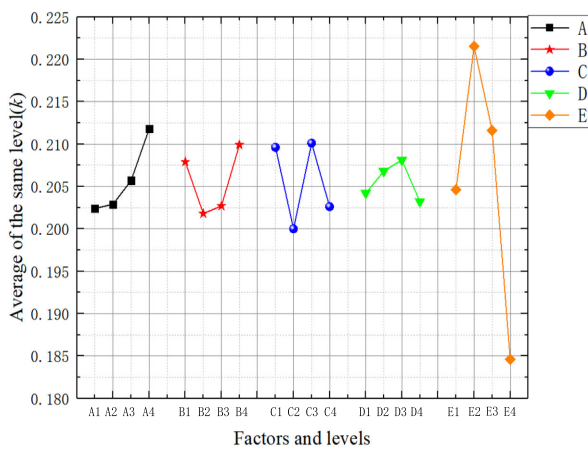


FIGURE 6. Level average and factor level diagram.

With regard to the topology optimization of frame, RI indicates the random consistency index and the specific value can be referred in Table 7. CR less than or equal to 0.10 is considered acceptable. If CR is larger than 0.10, the problem should be re-analyzed and the judgments are revised.

TABLE 7. Random consistency index.

N	1	2	3	4	5	6	7	8	9
RI	0	0	0.58	0.90	1.12	1.24	1.32	1.41	1.45

The weight coefficients of four working conditions, including bending, torsion, braking and turning, in the static stiffness, are determined first. According to Table 6, the relative importance ratio between each working condition is derived, and the matrix M is established:

$$M = \begin{bmatrix} 1 & \frac{1}{2} & 2 & 3 \\ 2 & 1 & 3 & 5 \\ \frac{1}{2} & \frac{1}{3} & 1 & 2 \\ \frac{1}{3} & \frac{1}{5} & \frac{1}{2} & 1 \end{bmatrix} \quad (16)$$

The maximum eigenvalue  $\lambda_{\max} = 4.016$  and corresponding eigenvector  $\omega = (0.548, 0.974, 0.316, 0.178)^T$  of the judgment matrix are obtained from the Eq. (8), (9) and (10). According to Eq. (12) and (13), the CR value of matrix M can be calculated to be 0.0519. Since  $CR = 0.0519 < 0.1$ , the constructed matrix meets the consistency criteria. By normalizing the elements in the eigenvector  $\omega$ , the weight ratios of the four stiffness conditions in multi-objective topology optimization of the frame can be obtained: 0.272, 0.483, 0.157 and 0.088. Similarly, a matrix can be established as shown below in term of the weight ratio between static stiffness and dynamic frequency:

$$M_{sd} = \begin{bmatrix} 1 & 2 \\ \frac{1}{2} & 1 \end{bmatrix} \quad (17)$$

It can be seen from the values of the elements in the matrix  $M_{sd}$  that the matrix is a consistent matrix because of the elements in the matrix meeting  $a_{ij} \cdot a_{jk} = a_{ik}$ . Therefore, there is no need for matrix  $M_{sd}$  to make consistency judgment. According to the above steps, the weight ratio between static stiffness and dynamic frequency can be calculated as: 0.585, 0.415. To sum up, the weight coefficients of each working condition in the multi-objective topology optimization of the frame obtained by the analytic hierarchy process are:  $\omega_{AHP1} = 0.272, \omega_{AHP2} = 0.483, \omega_{AHP3} = 0.157, \omega_{AHP4} = 0.088, \omega_{AHP} = 0.667$ .

Substituting the above two sets of weights into Eq. (12) yields a new set of weight ratio combination:  $\omega_1 = 0.182, \omega_2 = 0.378, \omega_3 = 0.26, \omega_4 = 0.18, \omega = 0.634$ . The three sets of weights obtained by three methods (shown in Table 8) are respectively put into the comprehensive optimization objective function to optimize the frame. The topological frame is shown in Figure 7 and the optimization iterative curve of different weight decision making methods is depicted in Figure 8. Compared with the single OTD method, the topology unit density obtained by the hybrid OTD + AHP method is more uniform over the entire frame, which can well display the approximate number and relative distribution position of the frame beam. Compared with the single AHP method, the obtained frame topology has better overall stiffness and dynamic frequency, which makes the frame structure clearer. Therefore, this greatly proves the rationality and correctness of the method by determining the proportion of weighting combined with subjective weighting and objective weighting. The scalability for the proposed decision making is very flexible. The proposed method is essentially a hybrid multi-objective decision-making method combining

TABLE 8. Three sets of weight ratio.

	$\omega_1$	$\omega_2$	$\omega_3$	$\omega_4$	$\omega$
OTD	0.091	0.273	0.363	0.273	0.600
AHP	0.272	0.483	0.157	0.088	0.667
OTD+AHP	0.182	0.378	0.260	0.180	0.634



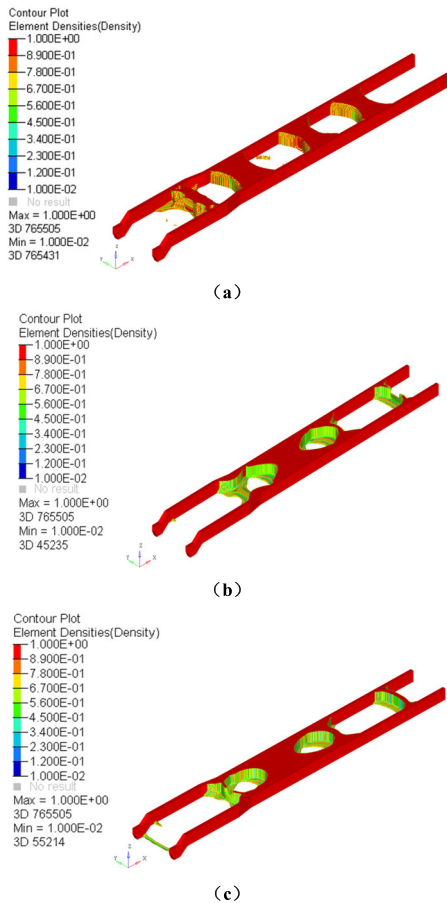


FIGURE 7. The topology results of the electric truck frame: (a) OTD method; (b) AHP method; (c) the proposed hybrid method.

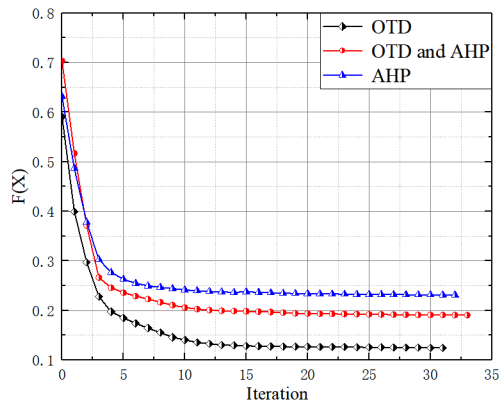


FIGURE 8. Topology optimization iterative curve of different weight decision making methods.

AHP and orthogonal table, so its greatest scalability lies in the adjustment of the weight distribution between the two methods. Strategic weight manipulation in multi-objective decision making makes it possible to solve a wider range of complex engineering problems.

According to the distribution of cell density in the frame topology shown in Figure 9, the number of beams and the relative arrangement position are determined. The specific

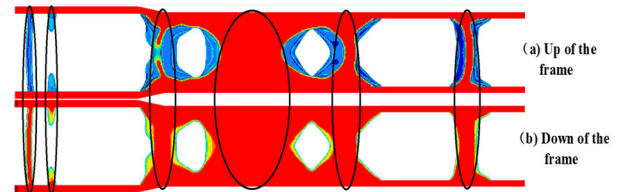


FIGURE 9. Density map of frame topological structure.

layout changes are shown in Figure 10. The new frame structure adjusts the layout of the frame beam and fully considers the load of the power battery pack on the frame. The new frame structure adjusts the arrangement of frame beams according to the result of frame optimization, and fully considers the load of the power battery pack on the frame.

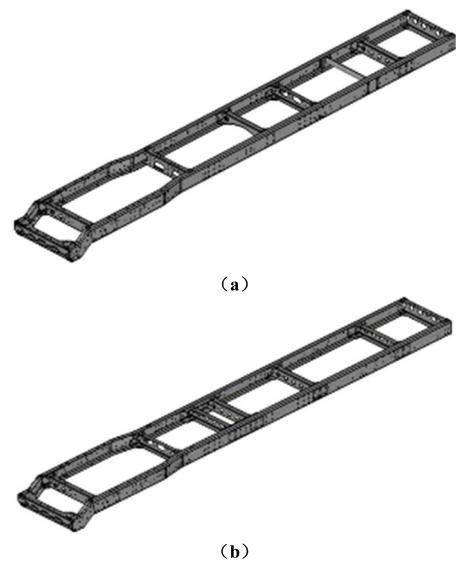


FIGURE 10. Comparison of the original frame and the new frame geometric mode: (a) original frame; (b) New frame.

### C. COMPARATIVE ANALYSIS

Figure 11 and Table 9 show the modal analysis data of original frame and new frame. It can be seen from the analysis results that the low-order natural frequencies of the new frame structure are improved except for the third order. The first-order frequency increased by 55.45%, and the

TABLE 9. Comparison of low-order natural frequencies.

No.	Original frame (Hz)	New frame (Hz)	Change%
First torsion	6.06	9.42	+55.45
Transverse bend	18.83	22.49	+19.44
Vertical bend	25.55	24.80	-2.94
Transverse bends	32.40	36.86	+13.77
Torsions	36.56	46.47	+27.11
Transverse bends	50.05	62.93	+25.73

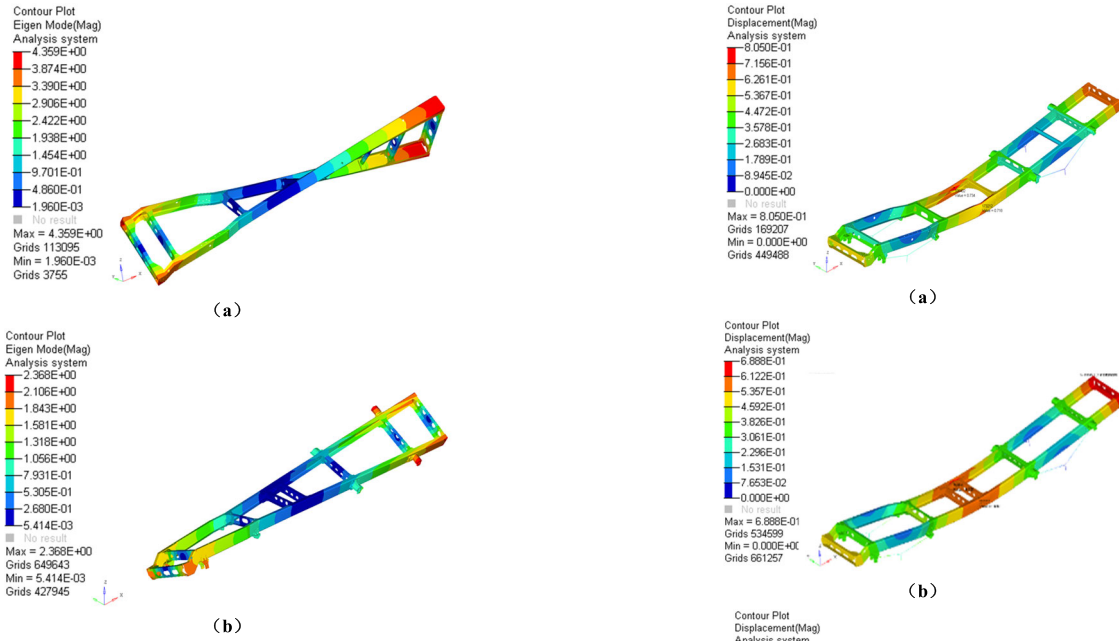


FIGURE 11. Comparison of the first mode of original and new frame: (a) original frame; (b) new frame.

TABLE 10. Comparison of stiffness analysis data.

Project		Original frame	New frame	Change%
Bending	Bending deflection (mm)	0.734	0.639	-12.94
	Bending stiffness (N/mm)	2724.80	3129.89	+14.87
Torsion	Torsion Angle (°)	0.238	0.25	+5.04
	Torsional stiffness (Nm/°)	5286	5032	-4.81

second-order frequency increased by 19.44%, and the fourth, fifth and sixth frequencies increased by 13.77%, 27.11% and 25.73% respectively. Moreover, the low-order frequency of the new frame structure can better avoid the external interference frequency, thereby avoiding the occurrence of resonance phenomenon.

Figure 12 and Table 10 show the stiffness analysis data of original frame and new frame. It can be seen that the bending rigidity of the new frame is increased by 14.87%. The main reason is that the arrangement of the fourth and fifth beams improves the bending rigidity of the new frame. The torsional

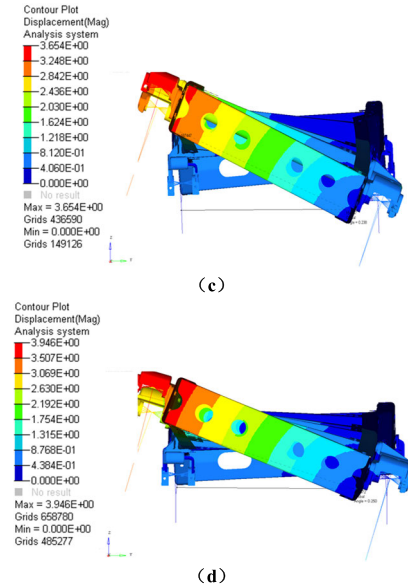


FIGURE 12. Comparison of the stiffness of original and new frame: (a) bending deflection of original frame; (b) bending deflection of new frame; (c) torsion angle of original frame; (d) torsion angle of new frame.

rigidity of the original frame is relatively high, because the sixth beam of the original frame is a cylindrical beam, which relatively increases the torsional rigidity of the original frame.

Table 11 shows the strength analysis data of original frame and new frame. From the data, the bending condition,

TABLE 11. Comparison of strength analysis data.

Project	Original frame			Optimal frame			Safety factor Change (%)
	Max stress	Max deformation	Safety factor	Max stress	Max deformation	Safety factor	
Bending	207.4	0.597	1.66	167.5	0.58	2.06	+24.10
Torsion	231.9	5.476	1.49	235.9	4.92	1.46	-2.01
Braking	204.1	0.599	1.69	198.4	0.77	1.74	+2.96
Turning	221.6	4.287	1.56	139.1	3.22	2.48	+58.97

the braking condition and the turning condition of the new frame structure are higher than the original frame except for the torsion condition. The strength of the structural frame is increased by 24.1%, 2.96% and 58.97% respectively. Although the strength of the new frame under torsional conditions is slightly lower than the original frame, the maximum strain displacement of the new frame is smaller than the original frame.

## V. CONCLUSION REMARKS

In this paper, multi-objective topological optimization developed by multi-objective decision-making method for an electric truck frame was thoroughly studied under various static and dynamic conditions. And a novel decision-making method for weight ratiocombining the OTD and AHP was proposed. Some remarkable conclusions could be summarized as follows:

(1) A novel decision-making method is proposed to determine the weight ratio in multi-objective optimization. It could be found that the frame optimized by the proposed hybrid method of determining the weight ratio is more reasonable than that of obtained by the respective corresponding method alone. And it also provides a reference with more insight information for studying the calculation of weight ratio of each sub-objective in multi-objective optimization. Since the method is a combination of subjective weighting method and objective weighting method, its calculation process may be somewhat complicated compared to other existing methods.

(2) From the single-objective optimization results, it could be seen that the rigidity of the frame structure under each different working conditions was significantly improved. However, it was only applicable for a given working condition and not the optimal solution under other operating conditions. In addition, it was quite difficult to determine the number and position of beams due to the uneven distribution of the existing unit structure of the frame.

(3) From the multi-objective optimization results, the optimal frame is superior to the original frame, which improved the utilization rate of the frame material and structural performance. In addition to the torsion condition and the third natural frequency, the strength and low-order natural frequency of the optimal frame had been significantly enhanced.

Therefore, the proposed multi-objective topology optimization method further developed by multi-objective decision-making can not only solve the frame optimization problem, but also expected to have certain theoretical guiding value and engineering practice reference value for multi-objective topology optimization of more complex engineering structure.

## ACKNOWLEDGMENT

The author Yongtao Liu would like to thank Prof. F. Xu at Wuhan University of Technology for providing suggestions and helpful discussions.

## REFERENCES

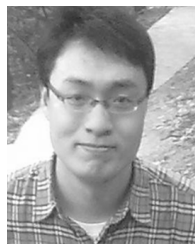
- [1] S. Lu, H. Ma, L. Xin, and W. Zuo, "Lightweight design of bus frames from multi-material topology optimization to cross-sectional size optimization," *Eng. Optim.*, vol. 51, no. 6, pp. 961–977, Jun. 2019, doi: 10.1080/0305215X.2018.1506770.
- [2] J. P. Blasques, "Multi-material topology optimization of laminated composite beams with eigenfrequency constraints," *Compos. Struct.*, vol. 111, pp. 45–55, May 2014, doi: 10.1016/j.compstruct.2013.12.021.
- [3] W. Chen and W. J. Zuo, "Component sensitivity analysis of conceptual vehicle body for lightweight design under static and dynamic stiffness demands," *Int. J. Vehicle Des.*, vol. 66, no. 2, pp. 107–123, Jan. 2014, doi: 10.1504/ijvd.2014.064546.
- [4] W. Zuo, "Bi-level optimization for the cross-sectional shape of a thin-walled car body frame with static stiffness and dynamic frequency stiffness constraints," *Proc. Inst. Mech. Eng., D, J. Automobile Eng.*, vol. 229, no. 8, pp. 1046–1059, Jul. 2015, doi: 10.1177/0954407014551585.
- [5] O. M. Silva, M. M. Neves, and A. Lenzi, "A critical analysis of using the dynamic compliance as objective function in topology optimization of one-material structures considering steady-state forced vibration problems," *J. Sound Vib.*, vol. 444, pp. 1–20, Mar. 2019, doi: 10.1016/j.jsv.2018.12.030.
- [6] G. G. Tejani, V. J. Savsani, S. Bureerat, V. K. Patel, and P. Savsani, "Topology optimization of truss subjected to static and dynamic constraints by integrating simulated annealing into passing vehicle search algorithms," *Eng. Comput.*, vol. 35, no. 2, pp. 499–517, Apr. 2019, doi: 10.1007/s00366-018-0612-8.
- [7] A. Kozikowska, "Multi-objective topology and geometry optimization of statically determinate beams," *Struct. Eng. Mech.*, vol. 70, no. 3, pp. 367–380, Apr. 2019, doi: 10.12989/sem.2019.70.3.367.
- [8] J. B. Q. Zuliani, M. W. Cohen, F. G. Guimarães, and C. A. S. Junior, "A multi-objective approach for multi-material topology and shape optimization," *Eng. Optim.*, vol. 51, no. 6, pp. 915–940, Jun. 2019, doi: 10.1080/0305215X.2018.1514501.
- [9] A. Aminzadeh, A. Parvizi, and M. Moradi, "Multi-objective topology optimization of deep drawing dissimilar tailor laser welded blanks; experimental and finite element investigation," *Opt. Laser Technol.*, vol. 125, May 2020, Art. no. 106029, doi: 10.1016/j.optlastec.2019.106029.
- [10] H. Li, X. Ding, F. Meng, D. Jing, and M. Xiong, "Optimal design and thermal modelling for liquid-cooled heat sink based on multi-objective topology optimization: An experimental and numerical study," *Int. J. Heat Mass Transf.*, vol. 144, Dec. 2019, Art. no. 118638, doi: 10.1016/j.ijheatmasstransfer.2019.118638.
- [11] M. Teimouri and M. Asgari, "Multi-objective BESO topology optimization for stiffness and frequency of continuum structures," *Struct. Eng. Mech.*, vol. 72, no. 2, pp. 181–190, Oct. 2019, doi: 10.12989/sem.2019.72.2.181.
- [12] G. Sun, D. Tan, X. Lv, X. Yan, Q. Li, and X. Huang, "Multi-objective topology optimization of a vehicle door using multiple material tailor-welded blank (TWB) technology," *Adv. Eng. Softw.*, vol. 124, pp. 1–9, Oct. 2018, doi: 10.1016/j.advengsoft.2018.06.014.
- [13] Z. Zhang, R. Chen, Z. Xu, Y. He, and W. Li, "Research on multi-objective topology optimization of vehicle suspension control arm," *Mod. Manuf. Eng.*, vol. 53, no. 4, pp. 114–121, Apr. 2017, doi: 10.3901/jme.2017.04.114.
- [14] Z. D. Li and M. Q. Wang, "Research on topology optimization design for continuum structures with multiple load cases," *Mod. Manuf. Eng.*, vol. 124, no. 9, pp. 70–73, Sep. 2008, doi: 10.16731/j.cnki.1671-3133.2008.09.007.
- [15] H. Qin and D. Yang, "Compromise programming approach with grey weight factor for structural topology optimization under multiple load conditions," *Chin. Quart. Mech.*, vol. 39, no. 2, pp. 280–293, Apr. 2018, doi: 10.15959/j.cnki.0254-0053.2018.02.006.
- [16] K. Kambayashi, N. Kogiso, and T. Yamada, "Multiobjective topology optimization for a multi-layered morphing flap considering multiple flight conditions," *Trans. Jpn. Soc. Aeronaut. Space Sci.*, vol. 63, no. 3, pp. 90–100, May 2020, doi: 10.2322/tjsass.63.90.
- [17] O. da Silva Smith, "Topology optimization of trusses with local stability constraints and multiple loading conditions—A heuristic approach," *Struct. Optim.*, vol. 13, no. 2, pp. 155–166, Apr. 1997, doi: 10.1007/bf01199235.
- [18] G. H. Yoon, "Topology optimization for nonlinear dynamic problem with multiple materials and material-dependent boundary condition," *Finite Elements Anal. Des.*, vol. 47, no. 7, pp. 753–763, Jul. 2011, doi: 10.1016/j.finel.2011.02.006.

- [19] G. Wang, D. Zhu, N. Liu, and W. Zhao, "Multi-objective topology optimization of a compliant parallel planar mechanism under combined load cases and constraints," *Micromachines*, vol. 8, no. 9, p. 279, Sep. 2017, doi: [10.3390/mi8090279](https://doi.org/10.3390/mi8090279).
- [20] B. Zhu, X. Zhang, and S. Fatikow, "A multi-objective method of hinge-free compliant mechanism optimization," *Struct. Multidisciplinary Optim.*, vol. 49, no. 3, pp. 431–440, Mar. 2014, doi: [10.1007/s00158-013-1003-9](https://doi.org/10.1007/s00158-013-1003-9).
- [21] W. Zuo and K. Saitou, "Multi-material topology optimization using ordered SIMP interpolation," *Struct. Multidisciplinary Optim.*, vol. 55, no. 2, pp. 477–491, Feb. 2017, doi: [10.1007/s00158-016-1513-3](https://doi.org/10.1007/s00158-016-1513-3).
- [22] N. Ryu, W. S. Song, and Y. Jung, "Multi-objective topology optimization of a magnetic actuator using an adaptive weight and tunneling method," *IEEE Trans. Magn.*, vol. 55, no. 6, Jun. 2019, Art. no. 7202504, doi: [10.1109/tmag.2019.2899893](https://doi.org/10.1109/tmag.2019.2899893).
- [23] R. T. Marler and J. S. Arora, "The weighted sum method for multi-objective optimization: New insights," *Struct. Multidisciplinary Optim.*, vol. 41, no. 6, pp. 853–862, Jun. 2010, doi: [10.1007/s00158-009-0460-7](https://doi.org/10.1007/s00158-009-0460-7).
- [24] Y. Sato, K. Izui, T. Yamada, and S. Nishiwaki, "Pareto frontier exploration in multiobjective topology optimization using adaptive weighting and point selection schemes," *Struct. Multidisciplinary Optim.*, vol. 55, no. 2, pp. 409–422, Feb. 2017, doi: [10.1007/s00158-016-1499-x](https://doi.org/10.1007/s00158-016-1499-x).
- [25] Jagadish and A. Ray, "Optimization of process parameters of green electrical discharge machining using principal component analysis (PCA)," *Int. J. Adv. Manuf. Technol.*, vol. 87, nos. 5–8, pp. 1299–1311, Nov. 2016, doi: [10.1007/s00170-014-6372-8](https://doi.org/10.1007/s00170-014-6372-8).
- [26] K. L. Wen, T. C. Chang, and M. L. You, "The grey entropy and its application in weighting analysis," in *Proc. IEEE Int. Conf. Syst., Man, Cybern.*, New York, USA, Oct. 1998, pp. 1842–1844.
- [27] A. K. Singh, S. Avikal, K. C. N. Kumar, M. Kumar, and P. Thakura, "A fuzzy-AHP and M-TOPSIS based approach for selection of composite materials used in structural applications," *Mater. Today: Proc.*, vol. 26, pp. 3119–3123, Jun. 2020, doi: [10.1016/j.matpr.2020.02.644](https://doi.org/10.1016/j.matpr.2020.02.644).
- [28] D. R. Jantos, C. Riedel, K. Hackl, and P. Junker, "Comparison of thermodynamic topology optimization with SIMP," *Continuum Mech. Thermodyn.*, vol. 31, no. 2, pp. 521–548, Mar. 2019, doi: [10.1007/s00161-018-0706-y](https://doi.org/10.1007/s00161-018-0706-y).
- [29] R. Ortigosa, D. Ruiz, A. J. Gil, A. Donoso, and J. C. Bellido, "A stabilisation approach for topology optimisation of hyperelastic structures with the SIMP method," *Comput. Methods Appl. Mech. Eng.*, vol. 364, Jun. 2020, Art. no. 112924, doi: [10.1016/j.cma.2020.112924](https://doi.org/10.1016/j.cma.2020.112924).
- [30] H. Qiao, S. Wang, T. Zhao, and H. Tang, "Topology optimization for lightweight cellular material and structure simultaneously by combining SIMP with BESO," *J. Mech. Sci. Technol.*, vol. 33, no. 2, pp. 729–739, Feb. 2019, doi: [10.1007/s12206-019-0127-2](https://doi.org/10.1007/s12206-019-0127-2).
- [31] Y. Zhang, M. Xiao, H. Li, L. Gao, and S. Chu, "Multiscale concurrent topology optimization for cellular structures with multiple microstructures based on ordered SIMP interpolation," *Comput. Mater. Sci.*, vol. 155, pp. 74–91, Dec. 2018, doi: [10.1016/j.commatsci.2018.08.030](https://doi.org/10.1016/j.commatsci.2018.08.030).
- [32] T. Iqbal, L. Wang, D. Li, E. Dong, H. Fan, J. Fu, and C. Hu, "A general multi-objective topology optimization methodology developed for customized design of pelvic prostheses," *Med. Eng. Phys.*, vol. 69, pp. 8–16, Jul. 2019, doi: [10.1016/j.medengphy.2019.06.008](https://doi.org/10.1016/j.medengphy.2019.06.008).
- [33] S. A. Khan and A. Mahmood, "Fuzzy goal programming-based ant colony optimization algorithm for multi-objective topology design of distributed local area networks," *Neural Comput. Appl.*, vol. 31, no. 7, pp. 2329–2347, Jul. 2019, doi: [10.1007/s00521-017-3191-5](https://doi.org/10.1007/s00521-017-3191-5).
- [34] J. Du and N. Olhoff, "Topological design of freely vibrating continuum structures for maximum values of simple and multiple eigenfrequencies and frequency gaps," *Struct. Multidisciplinary Optim.*, vol. 34, no. 2, pp. 91–110, Jun. 2007, doi: [10.1007/s00158-007-0101-y](https://doi.org/10.1007/s00158-007-0101-y).
- [35] P. Z. Zhou, J. B. Du, and Z. H. Lv, "Topology optimization of freely vibrating continuum structures based on nonsmooth optimization," *Struct. Multidisciplinary Optim.*, vol. 56, no. 3, pp. 603–618, Sep. 2017, doi: [10.1007/s00158-017-1677-5](https://doi.org/10.1007/s00158-017-1677-5).
- [36] D. Sui and Z. Cui, "Application of orthogonal experimental design and Tikhonov regularization method for the identification of parameters in the casting solidification process," *Acta Metallurgica Sinica (English Lett.)*, vol. 22, no. 1, pp. 13–21, Feb. 2009, doi: [10.1016/s1006-7191\(08\)60065-4](https://doi.org/10.1016/s1006-7191(08)60065-4).
- [37] A. Vild, S. Teixeira, K. Kuehn, G. Cuniberti, and V. Sencadas, "Orthogonal experimental design of titanium dioxide—Poly (methyl methacrylate) electrospun nanocomposite membranes for photocatalytic applications," *J. Environ. Chem. Eng.*, vol. 4, no. 3, pp. 3151–3158, Sep. 2016, doi: [10.1016/j.jece.2016.06.029](https://doi.org/10.1016/j.jece.2016.06.029).
- [38] W. S. Yang, F. Jona, and P. M. Marcus, "Application of orthogonal experimental design to LEED crystallography," *J. Vac. Sci. Technol. B, Microelectron.*, vol. 1, no. 3, pp. 718–722, Jul. 1983, doi: [10.1116/1.582587](https://doi.org/10.1116/1.582587).
- [39] J. Peng, F. Dong, Q. Xu, Y. Xu, Y. Qi, X. Han, L. Xu, G. Fan, and K. Liu, "Orthogonal test design for optimization of supercritical fluid extraction of daphnoretin. 7-methoxy-daphnoretin and 1,5-diphenyl-1-pentanone from *stellera chamaejasme* L. And subsequent isolation by high-speed counter-current chromatography," *J. Chromatography A*, vol. 1135, no. 2, pp. 151–157, Dec. 2006, doi: [10.1016/j.chroma.2006.08.099](https://doi.org/10.1016/j.chroma.2006.08.099).
- [40] E. B. Abrahamsen, M. F. Milazzo, J. T. Selvik, F. Asche, and H. B. Abrahamsen, "Prioritising investments in safety measures in the chemical industry by using the Analytic Hierarchy Process," *Rel. Eng. Syst. Saf.*, vol. 198, Jun. 2020, Art. no. 106811, doi: [10.1016/j.res.2020.106811](https://doi.org/10.1016/j.res.2020.106811).
- [41] D. Lee, D. Lee, M. Lee, M. Kim, and T. Kim, "Analytic hierarchy process-based construction material selection for performance improvement of building construction: The case of a concrete system form," *Materials*, vol. 13, no. 7, p. 1738, Apr. 2020, doi: [10.3390/ma13071738](https://doi.org/10.3390/ma13071738).
- [42] G. Marck, M. Nemer, J.-L. Harion, S. Russeil, and D. Bougeard, "Topology optimization using the SIMP method for multiobjective conductive problems," *Numer. Heat Transf., B, Fundamentals*, vol. 61, no. 6, pp. 439–470, Jun. 2012, doi: [10.1080/10407790.2012.687979](https://doi.org/10.1080/10407790.2012.687979).
- [43] G. Kiziltas, N. Kikuchi, J. L. Volakis, and J. Halloran, "Topology optimization of dielectric substrates for filters and antennas using SIMP," *Arch. Comput. Methods Eng.*, vol. 11, no. 4, pp. 355–388, Dec. 2004, doi: [10.1007/bf02736229](https://doi.org/10.1007/bf02736229).



**JIE QIAO** was born in Dali, Shaanxi, China, in 1988. She received the B.S. and M.S. degrees in vehicle engineering from Chang'an University, Xi'an, China, in 2011 and 2014, respectively, where she is currently pursuing the Ph.D. degree.

She holds ten academic articles and nine patents. Her research interests include lightweight design of vehicle structure and vehicle virtual test.



**FENGXIANG XU** was born in Xinxiang, Henan, China, in 1985. He received the B.S. degree in vehicle engineering and the Ph.D. degree in mechanical engineering from Hunan University, Changsha, China, in 2009 and 2015, respectively.

From 2015 to 2017, he was a Lecturer with the School of Vehicle Engineering. Since 2017, he has been an Associate Professor with the Hubei Key Laboratory of Advanced Technology of Automotive Components, Wuhan University of Technology, China. He is the author of more than 50 articles. He holds more than ten patents. His research interests include impact dynamics of materials and structures, lightweight design of vehicle structures, and engineering optimization method. He is also an Editorial Board Member of the journal *Advances in Engineering*. He is a Lead Guest Editor of the journal *Applied Computational Intelligence and Soft Computing*.



**KUNYING WU** was born in Henan, China, in 1992. He received the B.S. and M.S. degrees in vehicle engineering from the Wuhan University of Technology, Wuhan, China, in 2017 and 2019, respectively, where he is currently pursuing the Ph.D. degree.

He holds an academic article and six patents. His research interests include structure lightweight design and structural optimization.



**SUO ZHANG** received the M.S. degree in vehicle engineering from the Wuhan University of Technology, Wuhan, China, in 2020.

From 2018 to 2019, he was a Visiting Scholar with the Mechanical Engineering Department, The Hong Kong Polytechnic University, Hong Kong. His current research interests include optimization design methods for expensive black box functions, machine learning algorithms, bionic structural, and mechanical metamaterial design.



**YONGTAO LIU** was born in Dangshan, Anhui, China, in 1989. He received the B.E. degree in automobile service engineering and the M.S. and Ph.D. degrees in vehicle engineering from Chang'an University, Xi'an, China, in 2010, 2013, and 2015, respectively.

From 2013 to 2014, he was a Visiting Scholar with the University of Wisconsin–Madison. Since 2016, he has been a Lecturer with the School of Automobile, Chang'an University. He is the author of more than 30 articles. He holds 20 patents. His research interests include lightweight design of vehicle structures and intelligent vehicle control technology.

...